J. Fluid Mech. (1972), *vol.* 52, *part* 3, *pp.* 499–528
Printed in Great Britain

An experiment on the stability of small disturbances in a stratified free shear layer

By R. S. SCOTTI† AND G. M. CORCOS
Division of Fluid Mechanics, University of California, Berkeley

(Received 24 June 1971)

A statically stable stratified free shear layer was formed within the test section of a wind tunnel by merging two uniform streams of air after uniformly heating the top stream. The two streams were accelerated side by side in a contraction section. The resulting sheared thermocline thickened gradually as a result of molecular diffusion and was characterized by nearly self-similar temperature (odd), velocity (odd) and Richardson number (even) profiles. The minimum Richardson number J_0 could be adjusted over the range $0{\cdot}07 \leqslant J_0 \leqslant 0{\cdot}76$; the Reynolds number Re varied between 30 and 70. Small periodic disturbances were introduced upstream of the test section by a fine wire oscillating in the thermocline. The wire generated a narrow horizontal beam of internal waves, which propagated downstream and remained confined within the thermocline. The growth or decay of these waves was observed in the test section. The results confirm the existence of a critical Richardson number the value of which is in plausible agreement with theoretical predictions ($J_0 \simeq 0{\cdot}22$ for the Reynolds number of the experiment). The growth rate is a function of the wavenumber and is somewhat different from that computed for the same Reynolds and Richardson numbers, but the calculation assumed velocity and density profiles which were also somewhat different.

1. Introduction

In aerodynamics, the occurrence of turbulence is strongly associated with shear instability. While, of course, it is not true that only shear can destabilize a laminar flow, the theory of the stability of parallel flows describes substantially the circumstances under which we should expect to find turbulent flows. The same cannot be said of naturally occurring stratified flows. In the ocean and the atmosphere statically stable layers of fluid may be disturbed by a number of possible circumstances and it is not yet clear which types of perturbation engender nonlinear unsteady dynamics and macroscopic mixing. Whenever one associates a low Richardson number (large shear, small buoyancy) with an unstable flow one implicitly treats shear as a destabilizing parameter characterizing the undisturbed flow. However, shear may not be the primary or first cause of turbulence and mixing in many instances of stratified flows. Consequently an understanding of the circumstances under which mixing and turbulence are found in these flows may require also, or instead, a study of other sources of instability such as

† Present address: Woods Hole Oceanographic Institution, Woods Hole, Massachussetts.

the steepening of internal waves (from surface wave interaction, depth changes or other causes) or the formation of closed streamlines, a characteristic of the flow over even small obstacles of stratified fluid at low Froude and therefore usually high Richardson number. In both cases shear may play an important role, but it cannot properly be considered a parameter of the flow.

Nevertheless, the theory of the stability of infinitesimal disturbances in a flow which is statically stably stratified and sheared in a specified way has attracted the attention of a number of workers, starting with Thomson (1910). There exist adequate summaries of this theoretical work (e.g. Yih 1965; Drazin & Howard 1966). The work deals with a model of the mean flow which is two-dimensional and parallel. The disturbances which are introduced are supposed infinitesimal, inviscid† and periodic in the streamwise direction, with a complex exponential behaviour in time. Thus the disturbance stream function is assumed to be of the form $\psi = \phi(y)\, e^{i\alpha(x-ct)}$,

where α is real and $c = c_r + ic_i$ is complex. In much of the work the effect of density changes on inertia is neglected. Under these circumstances, the two parameters which appear in the differential equation for the disturbance are the wave-number α and the Richardson number

$$J(y) = \frac{g\, d\rho/dy}{\rho(dU/dy)^2},$$

where g is the gravitational constant, ρ the density, U the mean velocity and y the vertical co-ordinate. Some of the important conclusions of theoretical analyses made with these restrictions are:

(i) In order for a disturbance to grow in time ($c_i > 0$), the minimum Richardson number $J_0 < \frac{1}{4}$.

(ii) For such an unstable disturbance, the net complex velocity $c_r + ic_i$ (measured with respect to co-ordinates moving downstream with the arithmetic average of the maximum and the minimim mean velocity) is bounded by a semi-circle whose radius is $\frac{1}{2}\Delta U = \frac{1}{2}(U_{\max} - U_{\min})$.

(iii) If $c_i > 0$ it is bounded by

$$(\alpha c_i)^2 \leqslant \max\left\{\frac{1}{4}\left(\frac{dU}{dy}\right)^2 - \frac{g}{\rho}\frac{d\rho}{dy}\right\}.$$

(iv) Provided that $U(y)$ and $J(y)$ are analytic functions of y, a stability boundary is made of neutral modes for which $c_i = 0$ and U equals the wave velocity c_r somewhere. Unstable modes are contiguous neighbours of the stability boundary. (The proof requires some additional restrictions on the admissible class of velocity and density profiles.)

(v) There usually exist some neutrally stable internal gravity modes which are not part of the stability boundary and for which $c \neq U(y)$ everywhere. These are similar to the modes which exist in a fluid at rest.

These earlier results have been usefully complemented by recent work reported by R. E. Kelly and his associates. In one paper by Maslowe & Thompson (1971) both viscosity and heat conduction were taken into account in the numerical

† See, however, Koppel (1964), Gage & Reid (1968), Gage (1971) and Maslowe & Thompson (1971).

solution of the infinitesimal stability of a stratified free shear layer of the Holmboe type (i.e. one for which $U = 1+\tanh y$, $\rho = \exp(-\beta \tanh y)$. The neutral curve (a function of the wavenumber α and Reynolds number) was obtained for a range of J_0, and a Prandtl number = 0·72.

Two relevant experimental investigations of stability have come to our attention. One by Thorpe (1969, 1971) deals with immiscible as well as miscible fluids which are accelerated up or down a tilted tube. The second, by Clark (1969), was carried out in a water channel in which stratification was achieved by heating and in which observations were made of the natural occurrence of waves, of their wavelengths and of the Richardson number at which they occurred and at which they degenerated into non-periodic and into turbulent motion.

2. The choice of a mean flow

The experiment reported here related to the stability of free shear layers – idealizations of the shear flows found in oceanic thermoclines and estuaries. Such layers are typically well removed from boundaries, reasonably two-dimensional and have one or several inflexion points. Both in the ocean and in the laboratory, buoyancy may radically affect the evolution of the mean flow as well as its stability, so that it is difficult to select or to generate a typical profile. One may study the effect of buoyancy on the stability of specified velocity and density profiles only in so far as this effect and the effect of buoyancy upon mean-flow quantities can be made to depend on distinct parameters. It is not clear to what extent this state of affairs is typical of natural conditions. In practically all relevant theoretical studies of stability this point has been overlooked, and the mean velocity and density profiles have been chosen quite arbitrarily.

The experiment was designed in such a way that the effect of buoyancy upon the distribution of mean shear and mean density was negligible, while its effect upon the stability of the flow was controlling and nearly self-similar. The experimental flow was an approximation to the following model, considered by Schwember (1969).

Two streams, each with a vertically uniform velocity and density, are brought together at a streamwise station and the resulting discontinuity in mean velocity and in density diffuses downstream to form a shear layer and a thermocline of finite thickness. Call the streamwise component of mean velocity $U(x, y)$, the density ρ, the velocity and density of the upper stream $U_1(x)$ and ρ_1, and those of the lower stream $U_2(x)$ and ρ_2. Define $\overline{U}(x) = \frac{1}{2}(U_1+U_2)$, $\overline{\rho} = \frac{1}{2}(\rho_2+\rho_1)$ and $\Delta U = U_1 - U_2$, and assume $\Delta U/\overline{U} \ll 1$, $\Delta\rho/\overline{\rho} \ll 1$. For such a flow, even though, to first order in U, the density diffusion is unaffected by the velocity profile, J varies with x. However, it is possible to find self-similar velocity and density profiles $u = (U-\overline{U})/\Delta U$, $\theta = (\rho-\overline{\rho})/\Delta\rho$, provided that the inviscid interface is plane (which requires a large tunnel Froude number), and provided that $\overline{U}$ and ΔU vary as $x^{\frac{1}{5}}$. Then, assuming that density changes are due to heat, one finds that

$$u = g_1(\eta, Pr) + Dg_2(\eta, Pr),$$

where

$$\eta = \left(\frac{2gx^{\frac{1}{5}}}{\nu\overline{U}D}\right)^{\frac{1}{5}} \frac{y}{x^{\frac{2}{5}}} = \frac{\overline{U}_0^{\frac{1}{2}}}{x_0^{\frac{1}{10}}\nu^{\frac{1}{2}}x^{\frac{2}{5}}}y, \quad D = 2g\left(\frac{\nu x}{\overline{U}^5}\right)^{\frac{1}{2}},$$

$\overline{U}_0$ is a fixed reference velocity at location x_0, such that $\overline{U} = \overline{U}_0(x/x_0)^{\frac{1}{2}}$, and Pr is the Prandtl number $c_p\mu/k$; g_1 is an odd function of η (an error function) and, for values of Pr and D both of $O\{1\}$,† buoyancy adds a negative even contribution to g_1 which is of $O\{1\}$. For large values of Pr the effect of buoyancy remains of $O\{1\}$ only when D/Pr is $O\{1\}$. For this type of self-similar flow, $J(y = 0)$ is related to the parameter D by

$$D = (\epsilon J(0)/Pr^{\frac{1}{2}})^{\frac{2}{3}},$$

where $\epsilon = \Delta U/\overline{U}$, so that if the fluid is air it is possible to ensure that $D \ll 1$ and $J(0) = O\{1\}$, if $\Delta U/\overline{U} \ll 1$. For any value of D, since both D and ϵ are independent of x, $J(0)$ is independent of x and J is self-similar, i.e. $J = J(\eta, Pr)$. However for $D \ll 1$, $u \cong g_1(\eta)$ and $J(y = 0) = J_0$.

The conditions set forth above were generally satisfied. We discuss in §7 the extent to which they were not, in particular the anomalous growth of δ with x and the consequent variations with x of J_0.

In summary, then, the mean flow which the experiment approximates is one for which the density profile, the velocity profile and the Richardson number profile are all simple functions of $y/\delta(x)$ and δ is a gently increasing function of streamwise distance. It must be owned that even with a self-similar flow the variations of the local velocity and length scales of the layer introduce complications and uncertainties in the interpretation of the disturbance growth data. This is discussed in §6.

3. The design of a mean flow

The mean flow was created in a specially designed wind tunnel. The details of this design are given by Scotti (1969), and only a few of its salient features will be discussed here. The tunnel is of the open-return type. Air at room temperature enters through square bell-mouth into a settling area separated into two streams of equal size by a horizontal splitter plate. The top stream is heated uniformly and the bottom stream retains ambient temperature. The two streams merge at the end of the settling section and are accelerated side by side through a contraction section. Downstream, in the rectangular test section these two streams are separated by a narrow density gradient which coincides with a shear layer. The stratified shear layer remains horizontal through the test section and diffuses slowly with streamwise distance. The system is driven by a blower at the end of the test section (see figure 1 for a sketch of the facility).

The heating is done by two hot-water radiators; the water temperature is maintained by a small heat exchanger. At the exit of the second radiator the air temperature in the top channel is uniform and sensibly equal to that of the water. The top halves of the tunnel walls are then maintained at a temperature equal to that of the top stream by a water jacket. The bottom of the test section can be moved up or down so as to provide for small accelerations in the streamwise direction.

Large mailing tubes were provided upstream of the heater section in both

† Here, and throughout the paper, $O\{x\}$ should simply be taken as ' of magnitude comparable to that of x'.

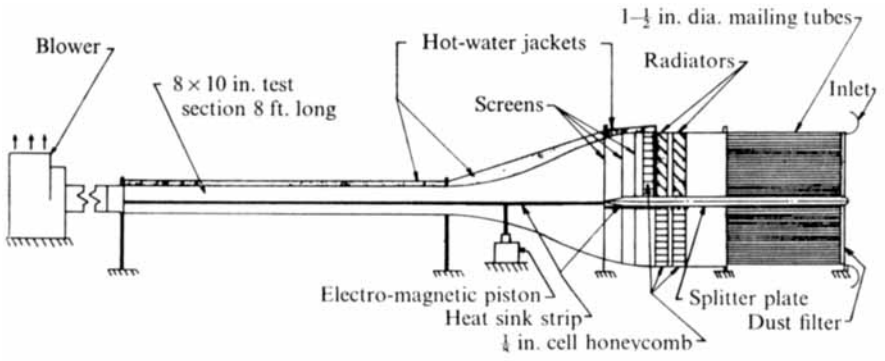

FIGURE 1. Sketch of the stratified flow tunnel.

channels. An $\frac{1}{8}$ in. cell honeycomb was installed downstream of the heater section. This honeycomb was meant to lower the disturbance level on top and to match the impedance of the radiators and top honeycomb to the bottom. Two fine mesh screens (36 mesh/in., 58 % open area) were used both to decrease flow inhomogeneities and turbulence and to help the boundary layer along the side walls to negotiate the contraction section (as seen in figure 1, the contraction of both top and bottom sections begins at the upstream screen). A third screen placed $\frac{3}{4}$ in. downstream of the trailing edge of the splitter plate serves the essential purpose of erasing the plate wake sufficiently to prevent shear instability of the wake in the contraction section (see figure 2).

The cross-sectional dimensions of the settling chamber are 36 × 36 in. Those of the test section are 8 in. (vertically) by 10 in. Radiative heating of the bottom half by the top half of the tunnel walls, not an altogether negligible effect, was limited by hand-rubbing the aluminium walls on top and coating the wooden bottom surfaces with aluminium foil.

Thermal characteristics of the tunnel

The temperature difference between the two streams was typically from 45–80° F, corresponding to fractional changes in density of 8–15 %. The slow temperature fluctuations of the heating water can be made smaller than $\pm 0{\cdot}5°$ F. The temperature differences in the water between inlet and outlet of the radiator or radiator and jacket water are smaller than 0·25° F. The bottom-wall temperature can be 4 or 5° in excess of the ambient temperature (a radiative effect), but it has been verified that, over the velocity range used, the bottom boundary-layer heating does not lead to gravitational instability or free convection up the side walls. The thermal turbulence level of the thermocline (the ratio of root-mean-square temperature fluctuation amplitude to total temperature difference between top and bottom layers) does not exceed 1 %.

Dynamic characteristics of the tunnel

It is possible to study the evolution of selected small perturbations only in a flow which is almost free of background disturbances. Conventional subsonic wind tunnels rely heavily upon the acceleration of the stream through a contraction to achieve this. For a stream with a vertical density stratification, passage through

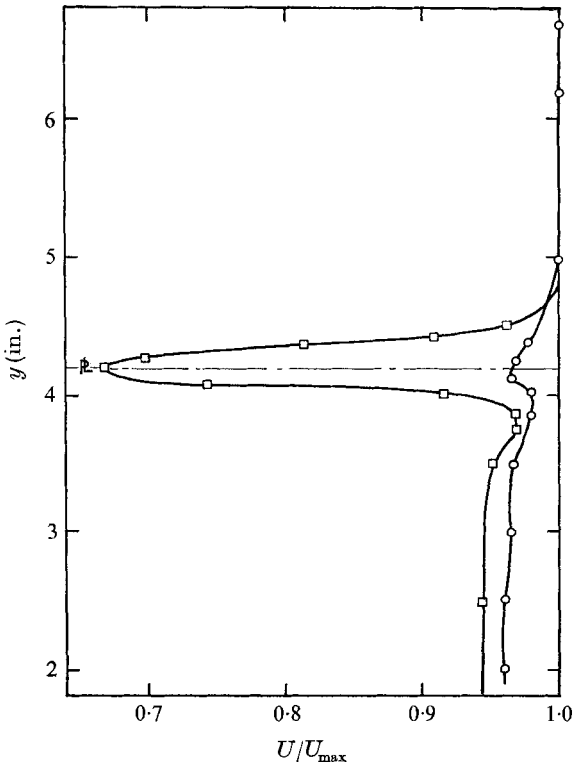

FIGURE 2. The effect of a screen on the velocity profile in the wake of the splitter plate. Probe $1\frac{3}{8}$ in. of trailing edge: □, no screen; ○, screen $\frac{3}{4}$ in. downstream, $Re_d = 6{\cdot}65$.

a contraction may, on the other hand, cause very large and unacceptable disturbances downstream. The theory of stratified flow through contractions is still largely undeveloped (see, however, Segur 1971) so that our wind tunnel was designed with the help of a crude analytical model. This is an inviscid one-dimensional two-layer channel flow which is enclosed by solid boundaries. The velocity of the top stream, U_1, and of the bottom stream, U_2, are functions of streamwise distance x only. The cross-sectional area of the channel is a function of x and the cross-sectional geometry is symmetric with respect to the horizontal mid-plane $\eta = 0$. The Bernoulli equation for each layer is used (no hydraulic jump is allowed) together with one-dimensional continuity for each stream and the condition that the pressure is vertically hydrostatic, and therefore continuous at the interface. The contraction may be horizontal (height constant), vertical (width constant) or square. The analysis is related to that performed by Long (1954) for a two-layer flow over a bump on a bottom wall. The results are qualitatively similar for all three classes of contractions. The two quantities of interest, the deflexion η of the interface relative to the half height and the velocity jump across the interface, depend on the reduced Froude numbers

$$F_1^2 = \rho_1 U_1^2/g\Delta\rho(h-\eta), \quad F_2^2 = \rho_2 U_2^2/g\Delta\rho(h+\eta),$$

where h is the local channel half-height. If $F_1^2 + F_2^2 > 1$ everywhere (supercritical flow), η has the sign required to decrease the local discrepancy between the two

Froude numbers (i.e. the interface deflects towards the stream with the lower Froude number). η increases with initial shear but η/h is always small after a sizeable contraction. If $F_1^2+F_2^2 < 1$ throughout the contraction, the interface deflexion tends to increase the discrepancy between local Froude numbers and even small contraction ratios may lead to large values of η.

For $F_1^2+F_2^2 = 1$, the interfacial slope is infinite (unless the channel has a throat) and there is no solution. Thus, according to one-dimensional theory smooth acceleration of two superposed layers of fluids of different density down a horizontal or vertical contraction is not possible unless

$$(F_1^2+F_2^2)_{\text{exit}} < 1 \quad \text{or} \quad (F_1^2+F_2^2)_{\text{entrance}} > 1.$$

Since this parameter varies rapidly with the contraction ratio C (i.e. faster than† C^2 for horizontal contractions, faster than $C^{2\cdot5}$ for square contractions, faster than C^3 for vertical contractions), this criterion seems to forbid a very large range of operating conditions; only initially supercritical or extremely subcritical flows would be possible. Experimental observations (see figures 3, 4 and 5, plates 1, 2 and 3) for different contractions, in which C was widely varied, were qualitatively consistent with the predictions of the simple theory. Whenever a 'choking' condition ($F = F_1^2+F_2^2 = 1$) was approached from above, the interface assumed the shape of a stationary wave of large amplitude and as F was further reduced a large, almost stagnant region was found to separate the two streams. For this and lower values of F, for which the flow remained profoundly disturbed, the thermal boundary conditions on the tunnel side walls were unsatisfactory and probably dominant; our observations were marred by free convection along the walls which introduced strong streamwise vorticity.‡ It is clear on more general theoretical grounds (e.g. Drazin 1961) that a flow down a horizontal contraction in which $F \ll 1$ throughout would lead in principle to insignificant deflexion of the interface. However, such a flow would have been unsatisfactory for several reasons, only one of which will be mentioned here; the shear layer developed between the two streams would have been deficient in shear (its Richardson number would have been too high for a stability experiment).

Thus the only satisfactory mode of operation was the supercritical mode, $F > 1$ throughout the contraction, which leads to large values of F in the test section. For adequate contraction ratios and almost uniform total pressure

† If h and w are the half-height and width of the channel and, h_0 and w_0 these quantities at an initial section, then $C \propto (w_0/w)$, $(h_0/h)^2$ or (h_0/h) for a horizontal, square or vertical contraction respectively. The inequalities are obtained for an initially subcritical flow for which the interface deflexion always increases the value of $(F_1^2+F_2^2)$. Then for $\eta = 0$,

$$(F_1^2+F_2^2) \sim (\rho_1 U_1^2+\rho_2 U_2^2)/h,$$

and U_1^2 and U_2^2 are related to h and w and therefore to C by one-dimensional continuity.

‡ There is a range of possible behaviour of real fluids, corresponding to the model postulated in the simple analysis, around a critical Froude number. If the fluid is thermally stratified the boundary conditions along the vertical walls are not compatible with two-dimensional flow. In addition, the fluid density differences are diffusive and regions of density intermediate between that of the two streams are created. These are the almost stationary bubbles which we observed. If the stratification is achieved by using two different and immiscible fluids at the same temperature such branching out of the interface is not possible, and either the boundary conditions are modified at upstream infinity (blocking) or hydraulic jumps occur (see Long 1954).

upstream, the velocity difference across the thin thermocline is primarily due to the different inertia of the two streams because η is very small and thus $(U_1/U_2)^2 \cong \rho_2/\rho_1$. Thus for a typical density ratio $\rho_2/\rho_1 = 1{\cdot}08$, $(U_1 - U_2)/U_2 \cong 0{\cdot}04$.

The fact that for a supercritical operation the total shear is a small fraction of the mean velocity has a number of important experimental consequences. The mean flow is then nearly unaffected by buoyancy while the fluctuations are not, a circumstance already mentioned as desired during the experiment. The characteristic time of growth of disturbances scales with $\delta/\Delta U$ but the disturbances propagate downstream at a rate $\cong \overline{U}$. Hence one must observe the growth rate over distances scaled with $\delta\overline{U}/\Delta U$, i.e. over many wavelengths. This is a disadvantage because over such distances mean quantities (e.g., $\overline{U}$ and δ) tend to change appreciably. Measuring the Richardson number (which involves the square of the velocity gradient) requires an unusually accurate determination of small velocity differences.

Turbulence level

Over the range of mean velocities used (11 to 18 ft/s) the turbulence level at the test section was less than 2×10^{-4} and uniform across the test section, excluding the wall boundary layers but including the central area downstream of the settling chamber splitter plate. Heating the upper stream did not change the turbulence level in the homogeneous regions of the flow. While background turbulence measurements were not undertaken within the thermocline itself, its turbulence level based, more appropriately, on ΔU was estimated from temperature fluctuation measurements to be of the order of $2 \times 10^{-4} U/\Delta U \cong 5^3 \times 10^{-3}$. It increased with streamwise distance and was a function of the Richardson number.

4. Generation of disturbances

For practical reasons, a small disturbance is always generated at a fixed station and it is its behaviour downstream of this station which is the object of observations, rather than its temporal behaviour everywhere (as assumed in the bulk of stability theory). In order for the stability problem to be well posed experimentally, the origin of the disturbance must be well confined in space. In our case, for instance, disturbing the free stream on either side of the sheared thermocline with an oscillating ribbon or airfoil results in a mixed experimental problem in which the shear layer oscillations grow partly as a result of instability and partly as a response to a forcing function along its entire length (in so far as the wake of the oscillator in the free stream is poorly damped). Thus the disturbances should be introduced within the shear layer, but the generator should not alter the mean flow of the shear layer–a very stringent requirement in our case since, for instance, a 1 % wake velocity defect would change the shear by about 20 %. Fortunately, the fact that the layer is stratified allows the generation of special disturbances with convenient properties. These are internal waves which can be generated upstream of the test section by the vertical oscillation of a very fine wire spanning the tunnel in the thermocline. The wire used was made of 0·004 in. diameter steel and strung between slides located in the side walls of the contraction section. It was activated by a large electromagnetic vibration exciter. The length of the

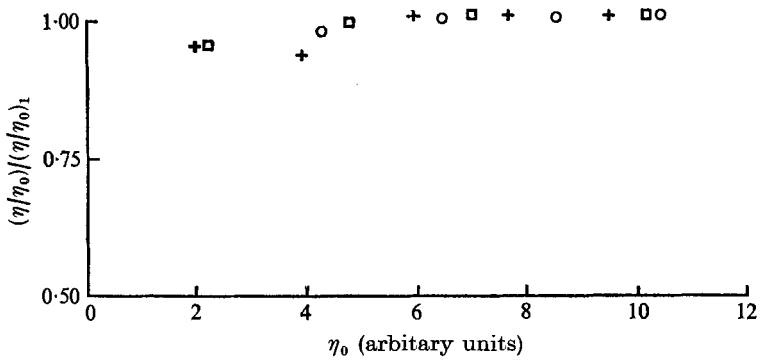

FIGURE 7. A check on the linearity of the disturbances.
+, 80·9 c/s; □, 39·7 c/s; ○, 20·0 c/s.

wire was about 18 in. and in so far as the maximum frequency required (about 200 c/s) was well below the pitch of the wire (about 700 c/s), the wire displacement was closely uniform and in phase along its total span. A subsequent analysis of the effect of an oscillating line force in a two-dimensional uniform density gradient and uniform velocity was made by Teuscher (private communication). It indicates that for the flow conditions and the frequency range of the experiment internal waves are propagated downstream within a beam originating at the wire and encompassing an angle of about 2°, so that the wave energy is entirely beamed downstream within the thermocline. The waves are eventually reflected by the varying density gradient and trapped within the thermocline. As they travel downstream they would tend to assume the structure of the (neutral) eigenmodes corresponding to the thermocline structure if there were no shear. In fact, they find themselves in a flow with a steadily decreasing Richardson number until they reach the test section. Thus they evolve progressively into instability waves.

It was determined that the wake of the wire was undetectable at the entrance to the test section, i.e. that the wake defect was less than $10^{-4}\overline{U}$. It was observed that the wire was unable to disturb any part of the flow in the test section unless it was vibrated within the thermocline. At the beginning of the test section, the maximum amplitude of the disturbance appeared to occur at the same relative position within the thermocline as that of the wire, a result which probably indicates, as suggested in Teuscher's computation, that the beam of internal waves had not spread beyond the central (uniform) part of the thermocline.

Friction in the dove-tailed slides to which the wire was attached caused the wire to be driven in a non-sinusoidal manner, i.e. it introduced higher harmonics of the motion (see figure 6, plate 4). These are apparent both from the output of the displacement transducer attached to the slides and from the temperature-fluctuation records measured at the entrance of the test section. However, these higher frequency components are generally outside the range of unstable modes and attenuate within a short distance, leaving a clean (sinusoidal) wave which grows or is attenuated at a slower rate.

The amplitude of the disturbances was chosen to be large enough for them to dominate background noise, but small enough for them to grow in a linear way. The linearity was assessed as shown in figure 7, a plot of the ratio of disturbance

amplitude at two streamwise stations against upstream amplitude. The wire displacement amplitude was of the order of two wire diameters, or 0·008 in. A typical wave displacement η was 0·004 in. for a wavelength of about 4 in.

5. Mean measurements

Temperature

The temperature of solid surfaces was measured with copper–constantan thermocouples and that of the stream by 10^{-4} in. diameter 10 % Rh–platinum wires operated at low current. For steady measurements involving large temperature differences the resistance was assumed to be a quadratic function of temperature. The constants were determined experimentally; temperature variations of 0·3° F could be detected. For fluctuation measurements, the relationship is linearized as

$$R_g = \gamma \bar{R}_g \theta,$$

where γ is the first coefficient of resistance, $\bar{R}_g$ the local mean wire resistance and θ the fluctuating temperature.

The wire is part of a constant current-system. Hence if e is the fluctuating voltage across the wire and I the current,

$$\theta = e/I\bar{R}_g\gamma.$$

Mean velocity

The determination of Richardson number requires the computation of the square of the local mean shear $\partial U/\partial y$. Since the total velocity variation is typically 4–5 % of the mean velocity an especially accurate method of measuring velocity variations had to be devised. The method used is an elaboration of the vortex-shedding cylinder method in which the frequency of vortex shedding of a long cylinder placed across the flow is related to the stream velocity. The relatively narrow range of velocities used and the fact that velocity and viscosity increase or decrease together during a traverse allow cylinders to operate over a narrow Reynolds number range. The range for which Roshko's (1954) Strouhal number–Reynolds number relationship is accurate (Tritton 1959; Webster 1964) turned out to be most desirable, both because it is a range for which the inherent uncertainty in shedding frequency is minimum and because it leads to cylinders whose diameter is small enough to give good spatial resolution (typically 8 or 10×10^{-3} in.). During a traverse the Reynolds number could always be confined to $50 \leqslant Re \leqslant 85$. The frequency of shedding was measured by a hot wire placed parallel to the cylinder axis and a few diameters downstream of it, and approximately one cylinder radius above or below the cylinder axis. The frequency of shedding, which was of the order of 2000 c/s, was measured by a counter and averaged over 1 or 10 s. The local temperature was also measured to determine the viscosity.

Such an arrangement typically yields fluctuations in recorded frequency of the order of 0·5–1 %. The corresponding uncertainty in the value of velocity is comparable. This is clearly excessive since, as was mentioned above, the maximum velocity variation at a given time is about 5 %. It was conjectured that the

uncertainty in shedding frequency was caused by small variations in the tunnel pressure which affected the velocity of the tunnel everywhere, at the same time and almost by the same amount. This led us to the use of a comparative method which consists of using two vortex shedders, one a stationary free-stream probe, the other a traversing probe, and reading directly the value of the ratio of the two shedding frequencies as well as the shedding frequency of the stationary probe. The theory of this comparative method is given in the appendix, and predicts that fractional errors in the measurement of the *difference* between free-stream and shear-layer velocity (if made as described) are of the same order as fractional errors in the measurement of free-stream velocity itself, while, of course, a conventional measurement would lead to fractional errors in velocity differences which would be greater by the factor $U/\Delta U$, i.e. about 25 times worse. The practice fully confirms the computations in that Reynolds number range. The signals from two similar shedding probes were fed simultaneously to an electronic counter which automatically yielded the ratio of their frequencies. This could be measured reproducibly to an accuracy of 2×10^{-4}. This result indicates not only that the cause of the small variations in shedding frequency was correctly identified, but also that, around a Reynolds number of 60, the shedding frequency is determined with remarkably little uncertainty by that parameter.†

Since the vortex shedder was used in flows which were both sheared and stratified, the effect of both of these features should be briefly discussed. It was determined experimentally that in the Reynolds number range used the effect of shear was to raise the shedding frequency, the fractional change in frequency being roughly equal to the value of the non-dimensional parameter $(d/U)\,(\partial U/\partial y)$. Typically this should lead to a maximum error (at the level of maximum shear) of $O\{0{\cdot}01\,\Delta U\}$ and to a negligible error in the value of the maximum slope $\partial U/\partial y$. No correction was provided for this error. The effect of stratification on shedding frequency should depend on the Froude number based on cylinder diameter, $[(gd^2/\rho U^2)\,(\partial\rho/\partial y)]^{-1}$, which is $O\{10^6\}$. Thus the stratification is likely to be far *too* weak to affect the shedding rate. Again the effect would be even smaller on the main quantity of interest, $(\partial U/\partial y)_{\max}$.

Finally, an internal joint check of the lack of importance of shear and density stratifications, as well as of the accuracy of Roshko's formula relating Strouhal number and Reynolds number, was performed by using cylinders of various sizes in and out of the sheared thermocline and verifying that they yielded the same velocity at the same point in space. Whatever errors occurred were random and did not exceed 0·5 %.

6. Disturbance measurements

In principle it is possible to measure the two velocity fluctuations u' and w', and the temperature fluctuations θ which are caused at any station in and about the shear layer by the passage of the wire-induced infinitesimal wave. One may record the streamwise rate of growth or decay of these fluctuations and infer from

† Additional measurements indicate that the root-mean-square of the deviation from a mean shedding frequency reaches a fairly sharp minimum at $Re = 60$.

these observations whether the disturbance is stable or unstable. In practice, one circumstance both limits the choice of the fluctuation which may be recorded with some accuracy and complicates the task of interpreting this or other measurements in terms of stability. The complicating factor is the large value of $U/\Delta U$. A hot-wire anemometer is sensitive both to temperature fluctuations and to velocity fluctuations and, when the fractional fluctuations in temperature and in velocity are of the same order, the hot-wire responds primarily to temperature fluctuations, even if it is operated at the maximum possible temperature. This is particularly true at the velocities which were typical of the experiment (the higher the velocity, the less sensitive a hot wire is to a given fractional change in velocity). Thus fluctuating velocity measurements would have been unacceptably inaccurate, and only temperature fluctuations were recorded by a hot-wire anemometer, operated at a low overheat ratio, at the mid-plane of the undisturbed thermocline.

The stability of disturbances and the streamwise growth of temperature fluctuations

For a mean flow which is unaccelerated and strictly parallel, one may characterize the stability problem by the exponential growth rate of the amplitude of one of several perturbed quantities such as the temperature fluctuation θ or the perturbed velocity components. When these are small, they all have the form

$$f_j(x, y, t) = g_j(y)\, e^{(\beta x - i\omega t)},$$

where β and ω have the same values for all indices j. The wavenumber is then the imaginary part of β and the spatial growth rate is the real part of β. A flow is unstable if $\beta_r > 0$ in the sense that the energy of the disturbance which is proportional to $\exp(2\beta_r x)$ is an increasing function of x. However, the experimental flow, while approximately self-similar, is x-dependent both because its thickness grows and because it is convectively accelerated. Under these circumstances, not only do the various perturbation quantities grow at different rates with x, but the identification of stability or instability with decay or growth of a given kind of disturbance is erroneous or at least inaccurate. In other words, the definition of a neutral disturbance is far from obvious.

Two problems should be distinguished. The first is that the theory of the stability of this type of self-similar mean flow does not apparently lead to an eigenvalue problem and is not available. At best one might expect that the amplitude of a quantity which is invariant for a neutral disturbance would grow approximately exponentially for an unstable case. This difficulty is not an experimental one and is not handled here, although a formal assumption of exponential growth rate is eventually made for purposes of comparison with the simple theory.

The second problem is that we are in need of a definition of a neutrally stable flow which can be translated in terms of measurable quantities. Such a definition was sought by analogy with other flows for which it is implicitly recognized that the non-uniform mean flow is energetically passive, i.e. that disturbances or waves merely propagate through it and that any apparent change in the disturbance energy is a result of viewing the disturbance in an accelerated reference frame.

Longuet-Higgins & Stewart (1960, 1961) and Whitham (1962) have discussed such cases involving surface water waves propagating through either longer waves or currents which are gradually non-uniform in the direction of propagation. The approach of Whitham, which seems to us to be the more fundamental, consists essentially of two steps.

First, mass, momentum and energy conservation laws are written for the total flow in integral form and the separation of the flow into mean quantities and fluctuating quantities is introduced into the conservation integral. This first step would evidently be identical in our case for neutrally stable, damped or unstable disturbances.

Second, the fluctuating quantities which appear in the conservation laws are evaluated from the second-order solution of the problem of propagation through a uniform medium (Stokes's waves). The corresponding task would be to evaluate these quantities from the neutral eigenfunctions of the stability problem in a parallel uniform flow. The result would be a first-order conservation statement for attributes of a neutral disturbance in a non-uniform flow. This result naturally depends on the type of mean-flow non-homogeneity which is present, and which is presumed known. Whitham gives several examples of this approach (some of which were previously treated by Longuet-Higgins & Stewart). For instance, for waves superposed on a free-surface flow $U(x)$ of varying depth $h_0(x)$ and continuity satisfied by inflow from below, the invariant obtained is

$$\frac{d}{dx}\{E(U+C_g)\}+S\frac{dU}{dx}=0,$$

where

$$S=E\left(\frac{2C_g}{C}-\frac{1}{2}\right), \quad E=\tfrac{1}{2}\rho g a^2,$$

E being the potential energy, a the wave amplitude, C_g the group velocity and C the wave velocity. To obtain a corresponding expression for the neutral eigenfunctions of the stability problems seems to be an ambitious undertaking because U is a function both of x and y, and because the eigenfunctions may have to be known to second order. Instead, we have made an admittedly inexact estimate of the error involved by defining as neutral disturbances those whose potential energy E (when averaged over a period) is independent of x. This was done by noting that for the various examples cited by Whitham S is of the order of E, so that for our case (for which $Cg \ll U$) the invariant probably has the form

$$\overline{U}\frac{dE}{dx}+\gamma E\frac{d\overline{U}}{dx}=0, \tag{6.1}$$

where γ is $O\{1\}$. We have then compared measured fractional changes in E for an unstable disturbance with fractional changes in $\overline{U}$ over the same length. The result is, fortunately, that for a typical unstable disturbance $\overline{U}$ varies decidedly less than E. For the lowest values of the Richardson number used ($J \cong 0{\cdot}07$), fractional changes in U are typically only 5 % of fractional changes in E, the maximum ratio occurring for large and small values of α for which the data reduction is also inaccurate on other counts. For $J \cong 0{\cdot}17$, the growth rates being less, the relative importance of the second term in (6.1) is greater (i.e. the growth rate

computation is more uncertain on a percentage basis), but the absolute value of the uncertainty in the true growth rate remains about the same. Thus it seems likely that the error involved in assuming that $dE/dx = 0$ defines a neutrally stable disturbance for the purpose of computing growth rates is tolerable and of the same order as, or smaller than, other experimental errors which are mentioned later. We note, however, that this error is systematic and tends to underestimate the growth rate of unstable disturbances (and to overestimate the decay rate of stable ones).

The data was thus reduced by assuming that the growth rate G was given by

$$G = \frac{1}{E}\frac{dE}{dx}.$$

Now, if P is the local average pressure, T the local average temperature, and $\tilde{T}$ and η the temperature and small vertical displacement of a particle above a level at which its temperature is T, the average disturbance potential energy is

$$E = \frac{gp}{2RT^2}\left(\frac{\partial T}{\partial y}\right)\overline{\eta^2},$$

where the overbar denotes a time average. We thus need to relate η to θ, the (measured) temperature fluctuation at a point. This is easily done if we assume that the temperature or density is only a weakly diffusive property of the fluid particles. Starting with an adequate approximation to the thermal equation:

$$\partial\tilde{T}/\partial t + (\tilde{U}.\nabla)\tilde{T} = \kappa\nabla^2\tilde{T}, \tag{6.2}$$

where $\tilde{T}$ is temperature, κ the thermal diffusivity, $\tilde{U}$ the velocity $(\tilde{U}, \tilde{V})$, and separating mean and fluctuating quantities:

$$\left.\begin{aligned}\tilde{T} &= T(x,y)+\theta(x,y,t),\\ \tilde{U} &= U(x,y)+u(x,y,t),\\ \tilde{V} &= V(x,y)+v(x,y,t),\end{aligned}\right\} \tag{6.3}$$

we linearize (6.2) after substitution of (6.3) and obtain

$$\frac{\partial\theta}{\partial t}+U\frac{\partial\theta}{\partial x}+V\frac{\partial\theta}{\partial y}+v\frac{\partial T}{\partial y}=\kappa\left[\frac{\partial^2\theta}{\partial x^2}+\frac{\partial^2\theta}{\partial y^2}\right]. \tag{6.4}$$

To the same approximation as is used in (6.4), the vertical velocity of a fluid particle is given in terms of its displacement η by

$$\frac{D\eta}{Dt} = v = \frac{\partial\eta}{\partial t}+U\frac{\partial\eta}{\partial x}. \tag{6.5}$$

If $$(u,\theta,\eta) = (u_0(y),\theta_0(y),\eta_0(y))\quad e^{(\beta x-i\omega t)},$$

then $v = \eta_0(U\beta - i\omega)$ and in the thermocline's plane of symmetry

$$\left[\theta_0+\eta_0\left(\frac{\partial T}{\partial y}\right)_{\max.}\right] = \frac{\kappa[(\partial^2\theta_0/\partial y^2)+\beta^2\theta_0]}{U\beta-i\omega}. \tag{6.6}$$

Now β is a complex quantity, $\beta_r + i\beta_i$, since in the experiment the disturbances grow or decay in space, rather than in time. Nevertheless it is easy to show that, for the case in which $\Delta U/\overline{U}$ is very small, the eigenvalue problem is formally

identical to that of a temporal stability problem except in the neighbourhood of $\beta_i = 0$, so that the general results of the temporal analysis (Miles 1963) can be used for order-of-magnitude evaluation. Thus

$$(\overline{U} - \omega/\beta_i)^2 + (\omega/\beta_r)^2 \leqslant \{\tfrac{1}{2}\Delta U\}^2 \tag{6.7}$$

and, writing the real and the imaginary parts of (6.6) separately and making systematic use of the inequality (6.7), we get

$$\mathrm{Re}\left\{\theta_0 + \eta_0 \left(\frac{\partial T}{\partial y}\right)_{\max}\right\} \cong \frac{\kappa}{\overline{U}\beta_r}\left[\frac{d^2\theta_i}{dy^2} - \beta_i^2\theta_i\right], \tag{6.8a}$$

$$\mathrm{Im}\left\{\theta_0 + \eta_0 \left(\frac{\partial T}{\partial y}\right)_{\max}\right\} \cong \frac{\kappa}{\overline{U}\beta_r}\left[\frac{d^2\theta_r}{dy^2} - \beta_i^2\theta_r\right]. \tag{6.8b}$$

We non-dimensionalize by using $\delta T = \Delta T/(\partial T/\partial y)_{\max}$ as a length scale and ΔU as a velocity scale. With $Pr = \nu/\kappa$, $Re_T = (\delta_T \Delta U)/\nu$, (6.8) becomes

$$\theta_r + \eta_r \left(\frac{\partial T}{\partial y}\right)_{\max} = O\left\{\frac{1}{Pr\,Re}\frac{\Delta U}{\overline{U}}\frac{1}{\beta_r \delta_T}\right\}\theta_i,$$

$$\theta_i + \eta_i \left(\frac{\partial T}{\partial y}\right)_{\max} = O\left\{\frac{1}{Pr\,Re}\frac{\Delta U}{\overline{U}}\frac{1}{\beta_r \delta_T}\right\}\theta_r,$$

where $\theta_0 = \theta_r + i\theta_i$. Thus if $Pr = O\{1\}$ and $Pr\,Re(U/\Delta U)(\beta_r \delta_T) \gg 1$, we can write approximately

$$\theta = -\eta(\partial T/\partial y)_{\max}. \tag{6.9}$$

Typically, $Pr\,Re\,(\overline{U}/\Delta U) \cong 800$ and $\beta_r \delta_T \cong 0{\cdot}1$, so that (6.9) is adequate for most of our measurements. Whenever $\beta_r \delta_T$ is found experimentally to be small, either because $\beta_i \delta_T$ is large or small or because J_0 is sufficiently large to allow only weak instability, little reliance can be placed on numerical estimates of growth rates which are based on the amplitude of θ. This is not believed to be a serious error for any of the data presented but may have been responsible for some scatter in some preliminary data taken around $J_0 = 0{\cdot}25$.

Determination of β_i, c_g and c

It is easy to determine β_i to sufficient accuracy. This follows from the fact that ω is measured directly and that according to the semicircle theorem

$$\overline{U} - c \leqslant (\tfrac{1}{2}\Delta U).$$

Hence the maximum error incurred in writing $\beta_i \cong \overline{U}/\omega$ is $\Delta U/2\overline{U}$, or about 2 %. A direct determination of β_i (by using two probes) verified its value in a few cases but was not more accurate. Since we devised no especially accurate means of measuring β_i directly, no value of either the phase velocity or the group velocity can be given; i.e. to our experimental accuracy, $c_g \cong c \cong \overline{U}$.

7. Experimental results: mean flow

Figure 8 shows a typical velocity and density profile at a given streamwise station. Successive non-dimensional profiles of temperature at different streamwise stations are shown in figures 9 and 10. Their close self-similarity is quite evident. The same is true of velocity profiles at almost all J_0 (figures 11, 12, 13).

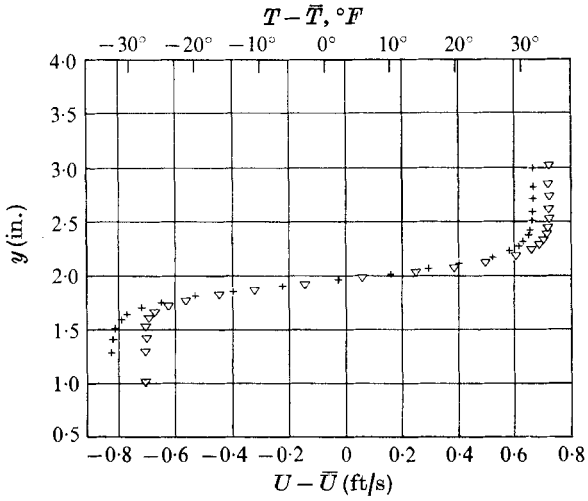

FIGURE 8. A typical set of mean profiles at a station. +, temperature; ▽, velocity.

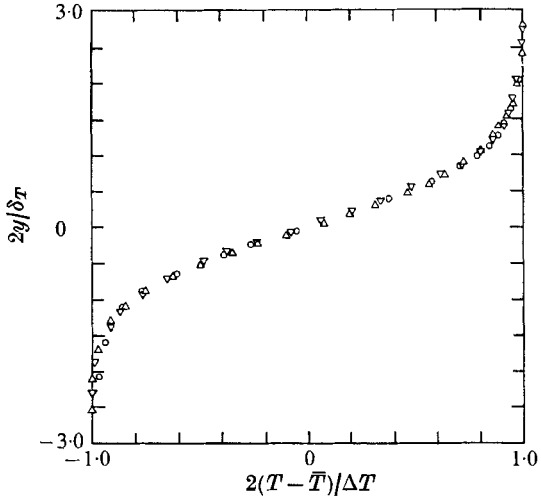

FIGURE 9. Check on self-similarity: temperature profiles at several streamwise stations.

	x (in.)	δ_T (in.)	J_0
○	12·0	0·413	0·070
▽	26·0	0·435	0·077
△	37·75	0·486	0·090

One notes, however, that some profiles deviate somewhat from the self-similar ones. It was verified that these relate to flow conditions for which the Froude number as defined in § 3 was most nearly critical at the beginning of the contraction section, where the two streams merge. In other words, the distribution of the velocity and temperature profiles in the test section was most likely the result of the distortion of the interfacial flow whenever the Froude number fell below a limiting value. For an air-heated tunnel this distortion is most likely to take the form of a stationary separated interfacial bubble which modifies the initial condition for the shear layer.

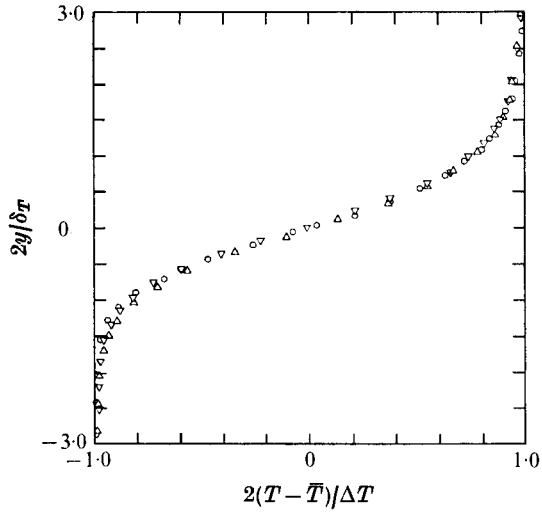

FIGURE 10. Check on self-similarity: temperature profiles at several streamwise stations.

	x (in.)	δ_T (in.)	J_0
○	12·0	0·437	0·151
▽	26·0	0·507	0·174
△	37·75	0·582	0·210

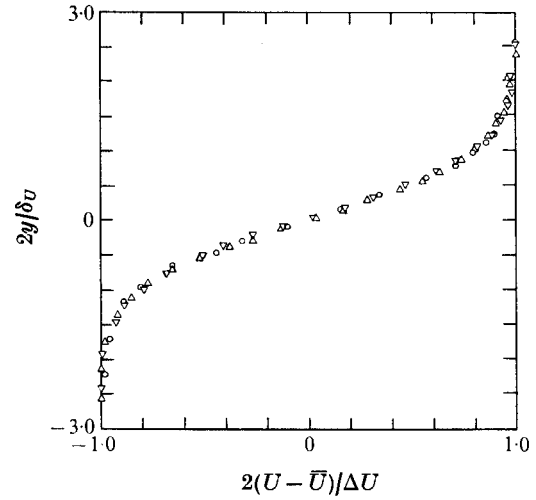

FIGURE 11. Check on self-similarity: velocity profiles at several streamwise stations.

	x (in.)	δ_T (in.)	J_0
○	12·0	0·398	0·070
▽	26·0	0·426	0·077
△	37·75	0·488	0·090

We have stated that if the mixing layers originated from a sharp discontinuity in mean velocity and mean density between two uniform streams, both density and velocity profiles would in theory be described by an error function (provided that $\Delta U/U \ll 1$). Figure 14 shows that such a function is a good approximation to the profile.

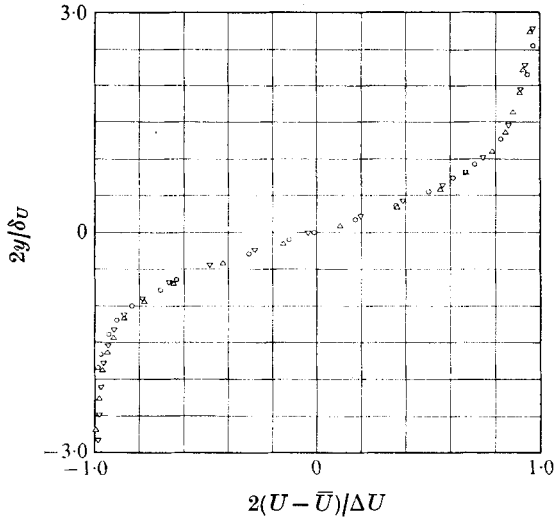

FIGURE 12. Check on self-similarity: velocity profiles at several streamwise stations.

	x(in.)	δ_T(in.)	J_0
△	12·0	0·410	0·151
▽	26·0	0·445	0·174
○	37·75	0·548	0·210

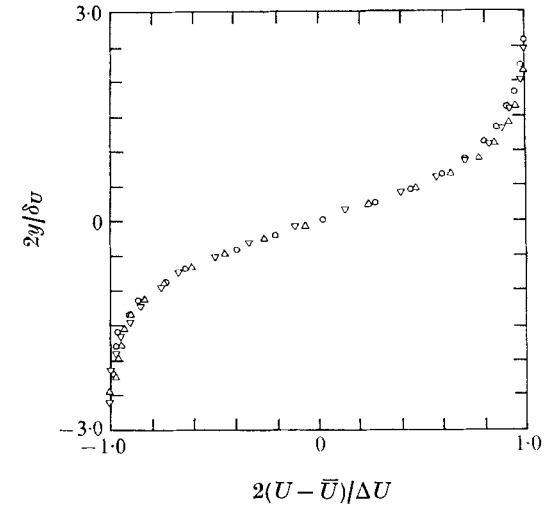

FIGURE 13. Check on self-similarity: velocity profiles at several streamwise stations.

	x(in.)	δ_U(in.)	J_0
△	12·0	0·422	0·260
▽	26·0	0·431	0·240
○	37·75	0·476	0·260

Richardson number distribution

Several vertical distributions of Richardson numbers are shown in figures 15 and 16. They are characteristically flat around $y = 0$ and this is also typical of the theoretical J distribution. For all of them, J_0 (the minimum value of J) is found to

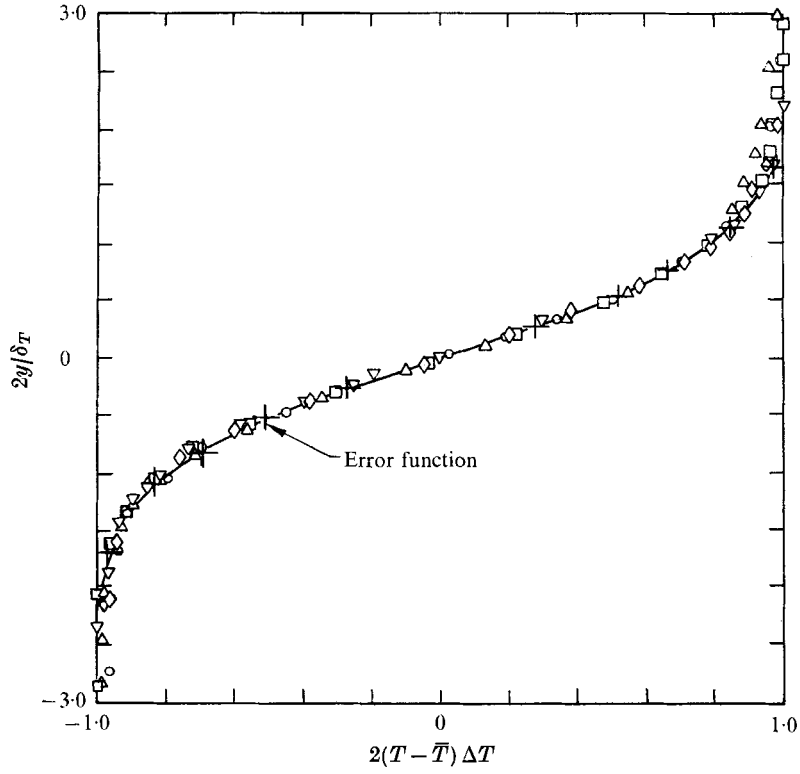

FIGURE 14. Temperature profiles: comparison with theory (error function).

	x (in.)	δ_T(in.)	J_0
○	12·0	0·497	0·460
▽	12·0	0·449	0·270
△	12·0	0·437	0·151
□	12·0	0·387	0·070
◇	12·0	0·413	0·070

be at $y = 0$, a result which one would expect from the theory for a gas ($Pr < 1$). In some cases, the distributions are closely self-similar and symmetric, in others some asymmetry is present, no doubt because the initial mean height of the thermocline and that of the shear layer fail to coincide precisely.

The streamwise variation of J_0 (which ideally should be constant) is shown in figure 17. In general it is seen that the two free streams were not accelerated quite enough, especially downstream, to compensate for the growth of the mixing layers. This growth is shown in figure 18. One notes that δ_u and δ_T grow more than linearly with x, a result which is unexpected in view of the discussion of § 2. It was first assumed that this excessive growth rate of a clearly laminar shear layer was due to a lateral convergence of the thermocline as a result of its interaction with the side walls. It is not possible to rule out such an interaction, but a direct measurement of the horizontal contraction of streamlines in the thermocline† failed to show sufficient departure from two-dimensionality to explain the growth rate of the shear and of the thermal layers.

† Using a small weather vane with a mirror and a laser beam.

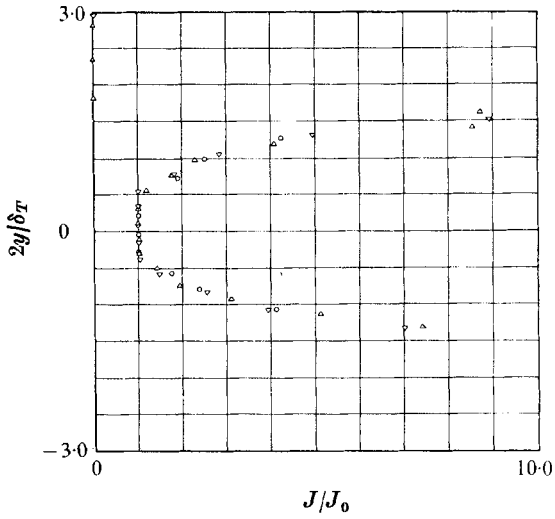

FIGURE 15. The Richardson number distribution.

	x (in.)	δ_T (in.)	δ_T (in.)	J_0
○	12·0	0·387	0·356	0·070
▽	26·0	0·438	0·408	0·071
△	37·75	0·513	0·483	0·091

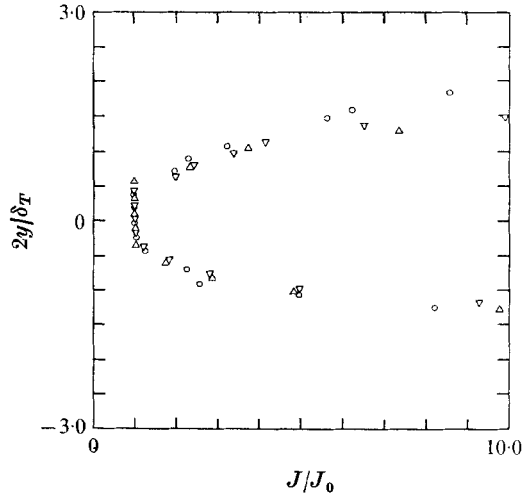

FIGURE 16. The Richardson number distribution.

	x (in.)	δ_T (in.)	δ_T (in.)	J_0
△	12·0	0·437	0·410	0·151
▽	26·0	0·479	0·431	0·174
○	37·75	0·507	0·470	0·210

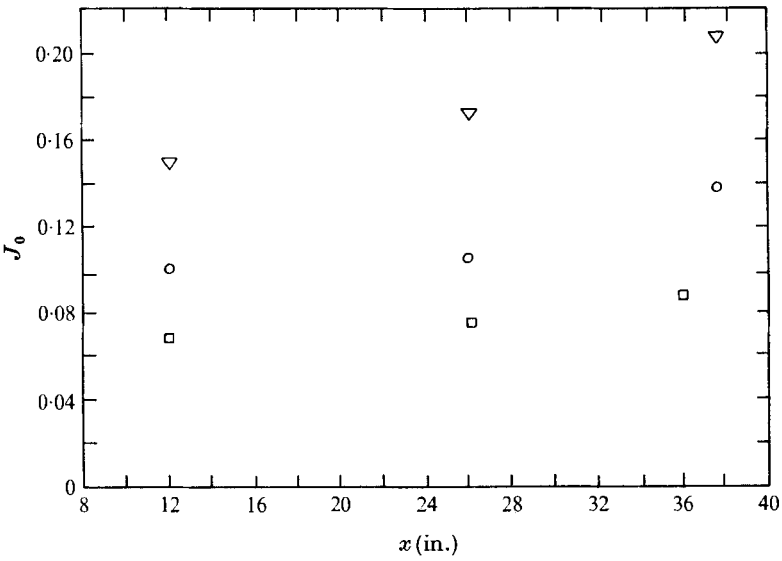

FIGURE 17. The distribution of minimum Richardson number with streamwise distance.

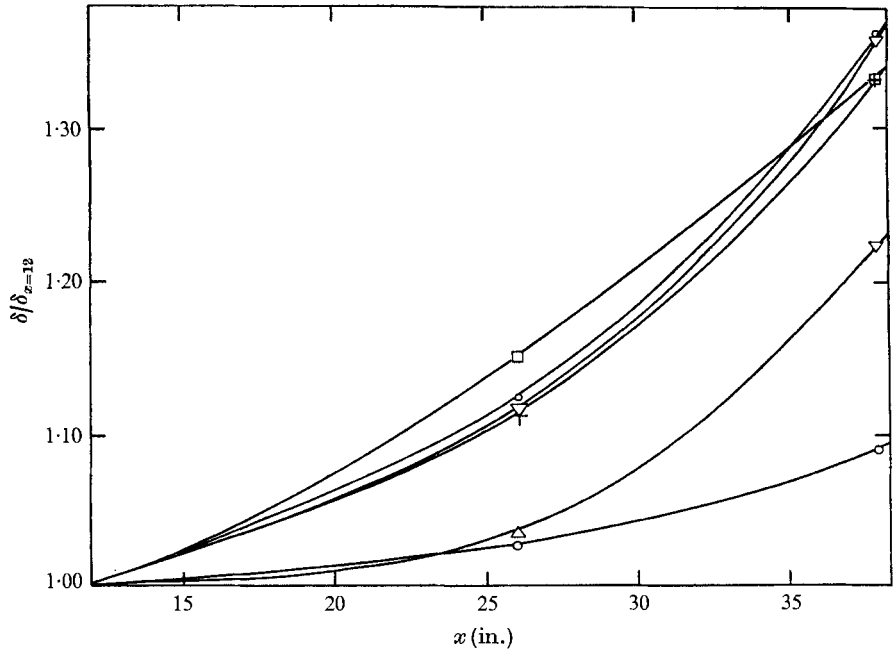

FIGURE 18. The distribution of thermocline thickness δ_T and shear layer thickness δ_U with streamwise distance. $\delta_T/(\delta_T)_{x=12}$: ○, $(\delta_T)_{x=12} = 0{\cdot}413$; +, $(\delta_T)_{x=12} = 0{\cdot}387$; □, $(\delta_T)_{x=12} = 0{\cdot}437$. $\delta_U/(\delta_U)_{x=12}$: △, $(\delta_U)_{x=12} = 0{\cdot}398$; ▽, $(\delta_U)_{x=12} = 0{\cdot}356$; ◯, $(\delta_U)_{x=12} = 0{\cdot}401$.

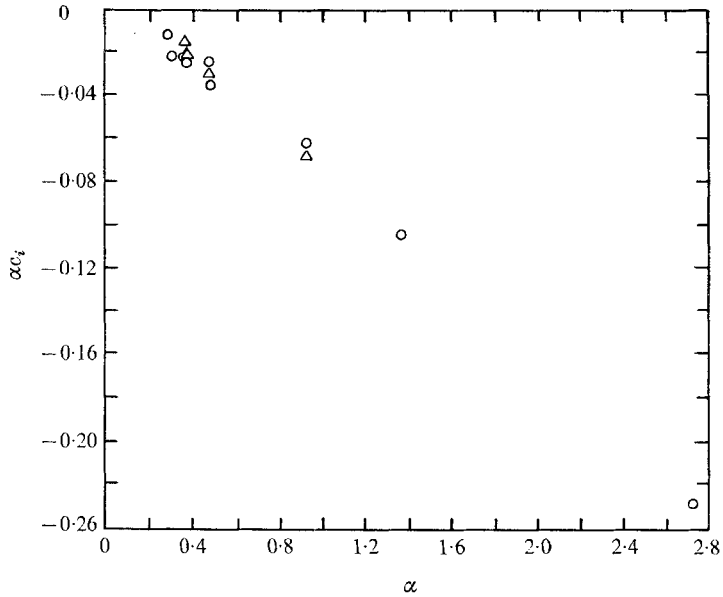

FIGURE 19. Decay rates for stable cases $J_0 > 0{\cdot}25$. ○, $J_0 = 0{\cdot}715$. $Re = 30$; △, $J_0 = 0{\cdot}47$, $Re = 31$.

8. Stability measurements

For Richardson numbers such that $0{\cdot}45 \leqslant J_0 \leqslant 0{\cdot}76$, all disturbances which were introduced (for which $0{\cdot}15 \leqslant \alpha \leqslant 2{\cdot}8$) were found to be attenuated (in the sense of §5) as they travelled down the test section. In terms of the temporal theory, the decay rates αc_i were independent of J_0, as shown in figure 19.

It was found that when $J_0 < \frac{1}{4}$, the energy of disturbances increased with streamwise distance within a narrow range of α. At values of J_0 which were very close to $\frac{1}{4}$, the measurements were scattered, the growth or decay rate of E was small and the data reduction procedure was evidently not sufficiently accurate. At smaller values of J_0 growth rates were better defined and the range of unstable wavelengths increased. Table 1 and figure 20 summarize the growth rate for three values of J_0 according to a temporal growth interpretation. These values were obtained from measurements of θ and $\partial T/\partial y$ at several streamwise stations from which E can be calculated by the method discussed in §6. The relationship between the time rate of growth of the disturbance energy E and the growth c_i is assumed to be given by

$$\frac{1}{\overline{E}}\frac{\partial E}{\partial t} \simeq \frac{\overline{U}}{\overline{E}}\frac{\partial E}{\partial x} \simeq 2\beta_i c_i,$$

where, in view of the large value of the ratio $\overline{U}/\Delta U$, no distinction need be made between $\overline{U}$, c_r and the group velocity c_g. The data presented are non-dimensionalized with respect to the local shear thickness $\delta_u = \Delta U/(\partial U/\partial y)_{\max}$ and the shear ΔU; for instance, $\alpha = \beta_i \delta_u$. The Reynolds number is defined as $(\Delta U\, \delta_u)/4\nu$, as is the prevailing custom in theoretical computations (cf. Maslowe & Thompson 1971). The streamwise derivatives of fluctuation amplitude and of mean density

	f(c/s)	α	αc_i
Average $J_0 \cong 0{\cdot}076$			
	20	0·125	0·032
	29·9	0·186	0·0345
	49·5	0·307	0·0854
	69·6	0·434	0·133
	85·9	0·534	0·136
	101	0·630	0·134
	120	0·748	0·1315
	141	0·880	0·0935
	165·7	1·05	0·0446
Average $J_0 = 0.105$			
Data (*a*)	20	0·13	0·0145
	29·9	0·207	0·035
	39·6	0·275	0·062
	59·4	0·412	0·077
	81.0	0·561	0·090
	101·0	0·70	0·078
	121·2	0·84	0·082
Data (*b*)	29.9	0·207	0·038
	80·9	0·56	0·079
	120·5	0·835	0·0465
	150.7	0·40	0·0228
Average $J_0 \cong 0{\cdot}170$			
	25·05	0·198	−0·013
	39·70	0·310	0·013
	54·40	0·420	0·035
	69·60	0·540	0·053
	85·90	0·670	0·057
	140·8	1·10	0·002

TABLE 1. Growth rate for unstable waves

gradient are evaluated from the average of differences at several stations (three stations for most of the data, four for some). In no case was an inconsistency between such averages and individual differences larger than a reasonable root-mean-square reading error, so that no variation in the growth rate with streamwise location of the measurement can be inferred from the data.†‡

† This statement is at variance with a remark of Scotti (1969, p. 54). Scotti's data also contained some errors in the evaluation of the mean Richardson number.

‡ As noted before, because $\Delta U/\bar{U} \ll 1$ only a small growth rate is apparent over a wavelength. The disturbances remain small in the sense of linear theory at all measuring sections.

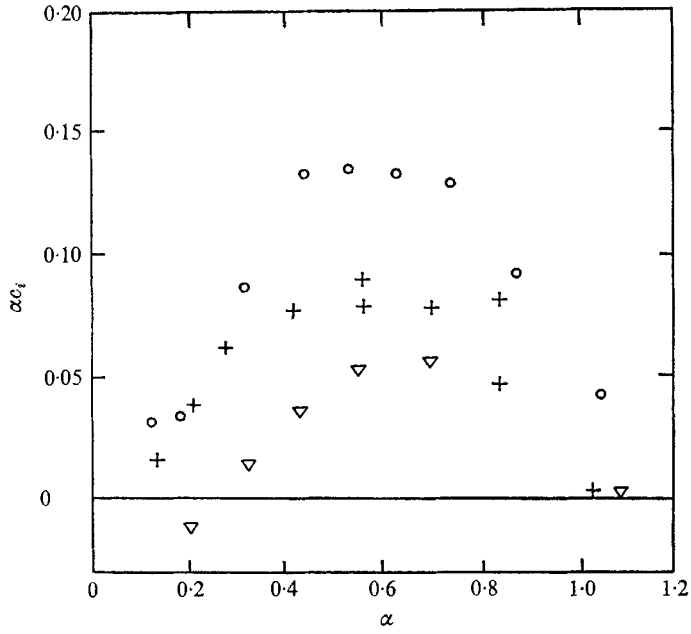

FIGURE 20. Growth rates for unstable cases $J_0 < 0{\cdot}25$. ○, $J_0 = 0{\cdot}076$, $Re = 54$; +, $J_0 = 0{\cdot}105$, $Re = 44$; ▽, $J_0 = 0{\cdot}17$, $Re = 33$.

9. Accuracy of the measurements

Scotti (1969) has provided an estimate of random errors for the mean and the fluctuating measurements.

Mean measurements

Fractional errors in mean velocity are given as 1 %, in mean velocity gradient as 3 % and in mean Richardson number as 8 %. The major source of uncertainty for the mean measurements is a slow variation of the temperatures of the top and of the bottom air layers.

Fluctuations measurements

Maximum fractional error in non-dimensional wavenumber is estimated at $\pm 1\,\%$ and that in reduced αc_i as $\pm 21\,\%$. In all cases where measurements were repeated, these estimates seemed to be quite conservative.

10. Comparison with theoretical predictions

In order to set the experimental results and the theoretical expectations side by side, we need to keep in mind some of the major features of the experiments which distinguish them from the models envisioned in the simplest theory, that for inviscid temporally growing disturbances in a sheared thermocline without horizontal boundaries and for which the Boussinesq approximation is made. These features are:

(i) The disturbances are growing spatially, not temporally.

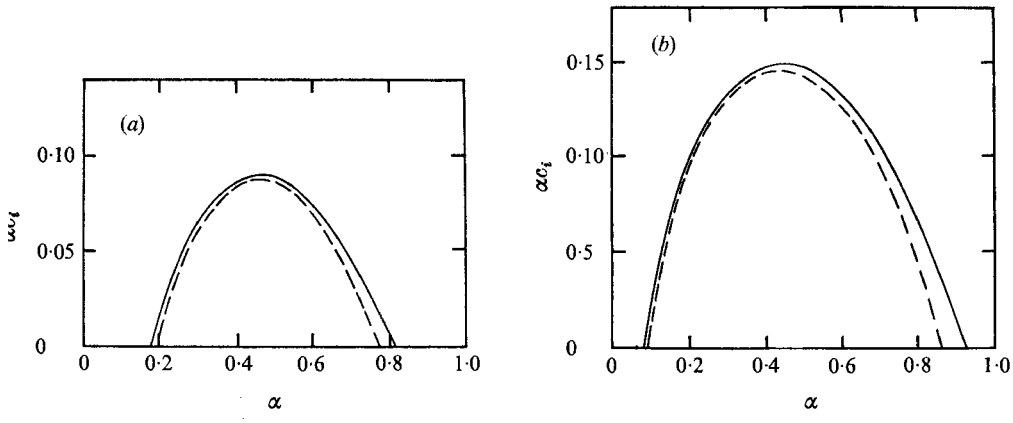

FIGURE 21. Comparison of theoretical growth rates for inviscid disturbances with hyperbolic tangent and with error function profiles (from Maslowe 1969). – – –, Holmboe function, ———, error function; (*a*) $J_0 = 0{\cdot}15$; (*b*) $J_0 = 0{\cdot}07$.

(ii) The Reynolds number of the experimental flow is relatively small ($30 < Re < 70$).

(iii) The flow has horizontal boundaries five inches above and below the thermocline.

(iv) The density variation across the layer is not very small.

The results of recent theoretical investigations concerning some of these complications are fortunately most probably applicable to our case, and we shall adapt these results to show that only feature (ii) above affected the experimental results enough to require theoretical correction.

To start with, Hazel (1972) has computed the temporal growth rates and the neutral curve for the simple parallel inviscid case when both the velocity and density profiles are error functions as in our case. He compared the neutral curve and the eigenvalues to those corresponding to the case of a hyperbolic tangent velocity and (logarithmic) density profiles. The comparison is also made by Maslowe (1969), for two values of J_0 typical of our experiment, in terms of the growth rate αc_i as a function of α. The results are encouragingly similar (figure 21) and suggest that conclusions reached for the Holmboe model should hold in our case.

(i) *Spatial vs. temporal growth*

In the experiment, an elementary unstable disturbance could be represented by

$$\psi(y, x, t) = \phi(y)\, e^{\beta x - i\omega t},$$

where β is complex and ω is real. Such an eigenvalue problem is formally different from that for which

$$\psi(y, x, t) = \phi(y)\, e^{i(\alpha x - ct)},$$

where α is real and c complex (the temporal problem). The spatial problem has been treated by Maslowe & Kelly (1971) but it would seem that the model they had in mind is not directly applicable to our case, because in the experiment $\Delta U/\overline{U} \ll 1$. In fact, it can easily be shown that if $\Delta U/\overline{U} \to 0$, and provided that the wave-number β_i is not too small, the differential equation for the spatial

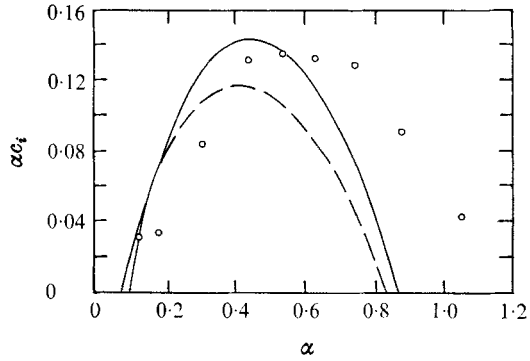

FIGURE 22. Growth rates for $J_0 \simeq 0{\cdot}076$. Comparison with theory for $J_0 \cong 0{\cdot}07$. ———, error function, $Re = \infty$; – – – –, Holmboe function, $Re = 53$; ○, experiment, $J_0 \cong 0{\cdot}076$, $Re \cong 54{\cdot}0$.

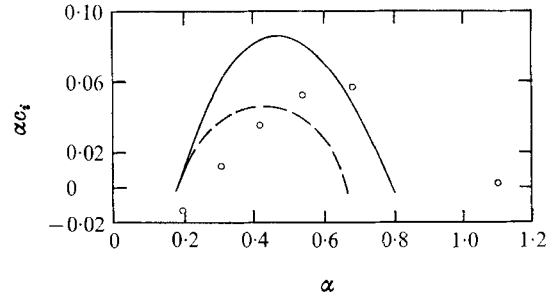

FIGURE 23. Growth rates for $J_0 \cong 0{\cdot}17$. Comparison with theory for $J_0 \simeq 0{\cdot}15$. ———, error function, $Re = \infty$; Holmboe function, $Re = 33$; ○, experiment, $J_0 = 0{\cdot}17, Re = 33$.

case tends to that for the temporal case with β_i^2 taking the role of α^2, and ω/β that of c. In the same limit, $\omega/\overline{U} \to \beta_i$. For the values of $\Delta U/\overline{U}$ typical of the experiment and omitting values of $\beta_i \delta_T \ll 1$ (say $\beta_i \delta_T < 0{\cdot}02$), which are excluded on other grounds as well, we should expect very close modelling from a temporal case.

(ii) *The effect of a finite Reynolds number*

Maslowe & Thompson (1971) have solved numerically the stability equations including the effects of both viscosity and heat conductivity on the (temporally growing) disturbance. The profiles were those of Holmboe. They find that at $Re = 50$, the critical $J_0 = 0{\cdot}22$. For $J_0 = 0{\cdot}15$ and $0{\cdot}07$, we have interpolated their plot of α *vs.* Re with c_i as a parameter to obtain curves of αc_i *vs.* α characteristic of the Reynolds numbers of the experiment. These plots are shown together with the experimental point in figures 22 and 23. In both cases the viscous correction is far from negligible.

(iii) *The effect of horizontal boundaries*

For all the data of the experiment, the ratio of the shear-layer thickness to its distance $\frac{1}{2}h$ from the top or the bottom wall is about one-tenth. Hazel (1972) has investigated numerically the effect of such boundaries, for the Holmboe case, on the shape of the stability boundary in the J_0, α plane. He finds that short waves

are stabilized and long waves destabilized by horizontal boundaries at a finite distance from the layer. The long-wave result is shown to be in accordance with the result of a simple solution for a discontinuous profile and density step (cf. Lamb 1932). However, for $h/2\delta = 10$, the short waves are unaffected and the stability boundary differs sensibly from that for unbounded space only for $\alpha < 0{\cdot}13$, a region for which, as we have seen, our data are really not credible on several grounds. Thus we conclude that the data presented is probably substantially free from systematic errors due to the finite vertical extent of the flow.

(iv) *The effect of finite density differences*

One may wonder whether the Boussinesq approximation which is made by Hazel (1972) in the computations which yield figure 21 is accurate enough for a flow wherein the density varies typically by 8 %. Maslowe (1969) gives numerical solutions of the stability equation for the case of zero buoyancy but finite (inertial) effects of vertical density gradient. His results, which are not numerically applicable to our case (since in the calculations $J_0 = 0$), nevertheless suggest that for a density change of 8 % (which in his terminology corresponds to a $\beta = 0{\cdot}04$) neither the rate of growth nor the range of unstable wavenumbers are appreciably affected. For instance, the spatial growth rate of the most unstable wave at $J_0 = 0$ is increased by about 2 %. Such an effect would be too small to be detected.

The plots of figures 22 and 23 suggest some systematic differences between the data and the viscous predictions of the temporal theory. The most significant one is that the growth rate curves are shifted to the right, i.e. that according to the experiment long waves grow somewhat slower and short waves faster than the theory predicts. Some (short) waves for which the theory indicates stability were found to grow. The maximum growth rate at a given Richardson number seems rather too large also, but in view of the uncertainty in data reduction, the discrepancy should not be taken too seriously. The distortion of the growth curves mentioned above may be due to rather small idiosyncrasies of the Richardson number distribution. It is known from the work of Miles (1963) and Hazel (1972) that the neutral curve is quite sensitive to relatively minor changes in the density distribution if these introduce an additional length scale. While our velocity and density profiles are likely to have only one inflexion point each, their maximum slope is not in general found at precisely the same height, and as a result the Richardson number distribution is not precisely symmetric. This was discussed in § 7.

A straight-line plot of $(\alpha c_i)_{\max}$ *vs.* J_0 (figure 24) gives an extrapolated value of 0.22 for the critical Richardson number. The theoretical value for the Holmboe profile at a Reynolds number of 50 is also about 0·22.

11. Conclusions

The results of the experiment confirm quantitatively, with satisfactory accuracy, the predicted effect of Richardson number upon the stability of small disturbances in a free shear layer. The growth rates are in crude agreement with predictions which take into account the effect of diffusion and viscosity upon the

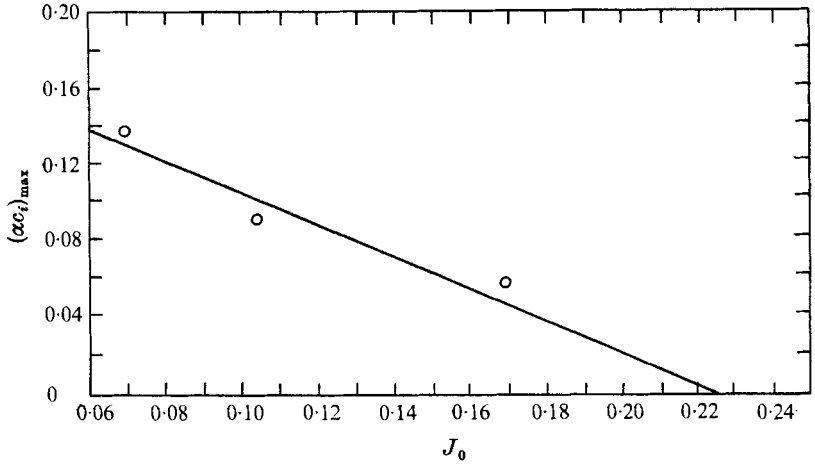

FIGURE 24. The inferred critical Richardson number. For this Reynolds number range, according to diffusive and viscous theory, the Holmboe profile is critical at $J_0 = 0{\cdot}22$, cf. Maslowe & Thompson.

dynamics of the disturbances. The accuracy of the growth rate data is not as high as one might wish but it is probably sufficient to suggest that the length of the most rapidly growing waves is noticeably affected by relatively minor variations in the mean density and velocity profiles.

The authors wish to thank Dr S. Maslowe, who graciously provided additional computations of growth rate for the viscous case, L. Teuscher for his analysis of the radiation pattern of the vibrating wire, H. Schwember for his study of the self-similar sheared thermocline, and F. S. Sherman for his collaboration in the study of two-layer inviscid one-dimensional flow in contractions, as well as for innumerable instances of help, support and patient listening. The work was financially supported by the Environmental Sciences Service Administration.

Appendix. The advantage of a dual-vortex shedding anemometer

We postulate that random variations in the shedding frequency of a measuring cylinder are mostly due to slow variations in the pressure drop between the end of the settling chamber and the test section. The static pressure is assumed independent of y.

Let the shedding frequency of a given cylinder be a slowly varying function of time:

$$f(y,t) = F(y)\,[1+\epsilon_f(t,y)].$$

Similarly, the pressure drop and the average of the top and bottom stream velocities are

$$\Delta p(t) = \langle \Delta p \rangle\,[1+\epsilon_p(t)], \quad \overline{U}(t) = \langle \overline{U} \rangle [1+\epsilon_{\overline{U}}(t)].$$

The brackets $\langle\,\rangle$ indicate a time average.

The cylinder shedding is quasi-steady and if the steady dependence of frequency on velocity is

$$F(y) = G(d, U, \nu)$$

then
$$\epsilon_f = \epsilon_U \frac{\langle U\rangle}{G}\frac{\partial G}{\partial U}.\dagger \tag{A 1}$$

Now when $\overline{U}$ varies, the velocity at a given y is affected both directly and indirectly (through variations in δ). Thus, in the limit of fluctuations in the self-similar layer of § 2, for which $\delta \sim \overline{U}^{\frac{1}{2}}$ and $\overline{U}$, ΔU_0 all vary in phase and by the small fractional amount $\epsilon_{\overline{U}}$, a Taylor series expansion of U around $\langle U\rangle$ leads to the result

$$U \cong \langle U\rangle + \epsilon_{\overline{U}}[U + \tfrac{1}{2}y\partial\langle U\rangle/\partial y].$$

The second term in the bracket vanishes for $y = 0$ and $y \to \pm\infty$, and in any case is of $O\{\Delta U/U\}$ compared with the first. Hence to order $\Delta U/U$, $\epsilon_U \cong \epsilon_{\overline{U}}$.

Since
$$\Delta p = \tfrac{1}{2}\overline{\rho}\overline{U}^2,$$
$$\epsilon_p = 2\epsilon_{\overline{U}}, \quad \epsilon_p \cong 2\epsilon_U. \tag{A 2}$$

Now consider two cylinders shedding simultaneously. The ratio of their frequencies f_1 and f_2 is given by

$$\frac{f_2}{f_1} = \frac{F_1\{1 + \tfrac{1}{2}\epsilon_p\,[(\langle U\rangle/G)\,\partial G/\partial U]_{y_1}\}}{F_2\{1 + \tfrac{1}{2}\epsilon_p\,[(\langle U\rangle/G)\,\partial G/\partial U]_{y_2}\}},$$

in view of (A 1) and (A 2). Alternatively

$$\frac{f_1}{f_2} = \left(\frac{F_1}{F_2}\right)\left\{1 + \tfrac{1}{2}\epsilon_p\left[\frac{d\ln G}{d\ln U}\right]_{y_2}^{y_1} + O(\epsilon_p^2)\right.,$$

but
$$[\partial \ln G/\partial \ln U]_{y_2}^{y_1} = \frac{\partial}{\partial U}(\partial \ln G/\partial \ln U)\,\delta U,$$

where δU is the velocity difference at the two points y_1 and y_2. Experimentally, $(\partial/\partial U)(\partial \ln G/\partial \ln U) \leqslant O\{1/\overline{U}\}$ for any Reynolds number. For the Reynolds number used it is approximately $0{\cdot}7/U$, so

$$\frac{f_1}{f_2} = \frac{F_1}{F_2}[1 + \tfrac{1}{2}\tau\epsilon_p\,\Delta U/\overline{U} + O\{\epsilon_p^2\}],$$

where $\tau = O\{1\}$. Hence fractional variations in f_1/f_2 are of $O\{\frac{1}{2}\tau\epsilon_p\,\Delta U/U\}$, while variations in f_1 or f_2 are of $O\{\epsilon_p\}$. To obtain $\langle \delta U\rangle$ we measure both f_2 (from which we compute U_2, a free-stream velocity) and f_1/f_2 directly. Then we find

$$\begin{aligned} f_1 - f_2 = f_2\left[\frac{f_1}{f_2} - 1\right] &= F_2[1+\epsilon_f]\left[\frac{F_1}{F_2}\left(1 + \frac{\epsilon_p}{2}\frac{\Delta U}{\overline{U}}\tau + \ldots\right) - 1\right] \\ &= (F_1 - F_2)\left[1 + \frac{\epsilon_p}{2}\tau + \frac{F_1}{F_1 - F_2}\epsilon_p\frac{\Delta U}{\overline{U}}\tau + \ldots O\{\epsilon_p^2\}\right] \\ &= (F_1 - F_2)\,[1 + O\{\epsilon_p\}] \end{aligned}$$

whereas, if the measurements of f_1 and f_2 are made separately,

$$f_1 - f_2 = (F_1 - F_2)\,[1 + O\{\epsilon_p\overline{U}/\Delta U\}].$$

In theory, the accuracy is thus improved by a factor of the order of 25.

† There is, however, an additional term: if $T = \langle T\rangle[1 + \epsilon_T]$, this term is

$$\epsilon_u \frac{\langle U\rangle}{G}\frac{\partial G}{\partial \nu}\frac{\partial \nu}{\partial T}\frac{\partial T}{\partial \eta}\frac{\partial \eta}{\partial U},$$

but it turns out to be small for the same reason as the corresponding velocity term (see next paragraph).

REFERENCES

CLARK, J. W. 1969 Laboratory investigation of atmospheric shear flows using an open water channel. *AGARD–NATO Meeting, Munich*, 15.

DAVIS, R. E. 1969 *J. Fluid Mech.* **36**, 337.

DRAZIN, P. G. 1961 *Tellus*, **13**, 239.

DRAZIN, P. G. & HOWARD, L. N. 1966 Hydrodynamic Stability of Parallel Flow of Inviscid Fluids. In *Advances in Applied Mechanics*, vol. 9 (ed. G. Kuerti). Academic.

GAGE, K. S. 1971 *J. Fluid Mech.* **47**, 1.

GAGE, K. S. & REID, W. H. 1968 *J. Fluid Mech.* **33**, 21.

HAZEL, P. 1972 *J. Fluid Mech.* **51**, 39.

KOPPEL, D. 1964 *J. Math. Phys.* **5**, 963.

LAMB, H. 1932 *Hydrodynamics*, 6th edn., p. 378. Dover.

LONG, R. R. 1954 *Tellus*, **6**, 97.

LONGUET-HIGGINS, M. S. & STEWART, R. W. 1960 *J. Fluid Mech.* **8**, 565.

LONGUET-HIGGINS, M. S. & STEWART, R. W. 1961 *J. Fluid Mech.* **10**, 529.

MASLOWE, S. A. 1969 A theoretical study of the stability of stratified shear layers. Doctoral dissertation, University of California, Los Angeles.

MASLOWE, S. A. & KELLY, R. E. 1971 *J. Fluid Mech.* **48**, 405.

MASLOWE, S. A. & THOMPSON, J. M. 1971 *Phys. Fluids*, **14**, 453.

MILES, J. W. 1963 *J. Fluid Mech.* **16**, 209.

ROSHKO, A. 1954 On the development of turbulent wakes from vortex streets. *N.A.D.A. Rep.* no. 1191.

SCHWEMBER, H. E. 1969 The interaction of buoyancy, shear and diffusion in stratified flows. *College of Engineering, University of California, Berkeley. Rep.* no. AS-69-2.

SCOTTI, R. S. 1969 An experimental study of a stratified free shear layer. *College of Engineering, University of California, Berkeley Rep.* no. AS-69-1.

SEGUR, H. 1971 *J. Fluid Mech.* **48**, 161.

THOMSON, W. 1910 *Mathematics and Physics Papers*, vol. 4, pp. 76–85. Cambridge University Press.

THORPE, S. A. 1969 *J. Fluid Mech.* **39**, 25.

THORPE, S. A. 1971 *J. Fluid Mech.* **46**, 299.

TRITTON, D. J. 1959 *J. Fluid Mech.* **6**, 547.

WEBSTER, C. A. G. 1964 *J. Fluid Mech.* **19**, 221–245.

WHITHAM, G. B. 1962 *J. Fluid Mech.* **12**, 135.

YIH, C.-S. 1965 *Dynamics of Nonhomogeneous Fluids*. Macmillan.

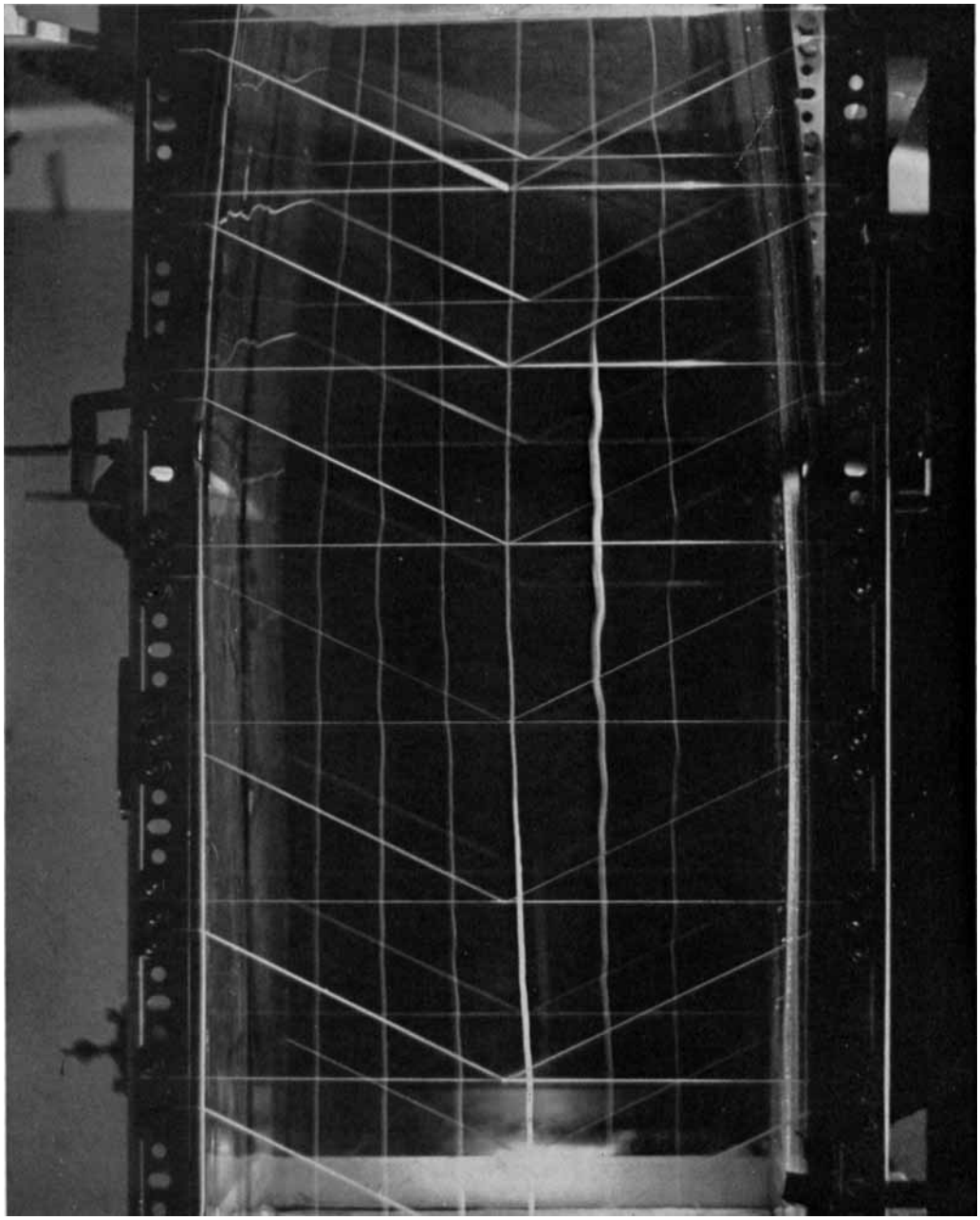

FIGURE 3. Stratified flow through a weak contraction. Supercritical flow: $(F_1^2 + F_2^2) \gg 1$ throughout (flow is from left to right).

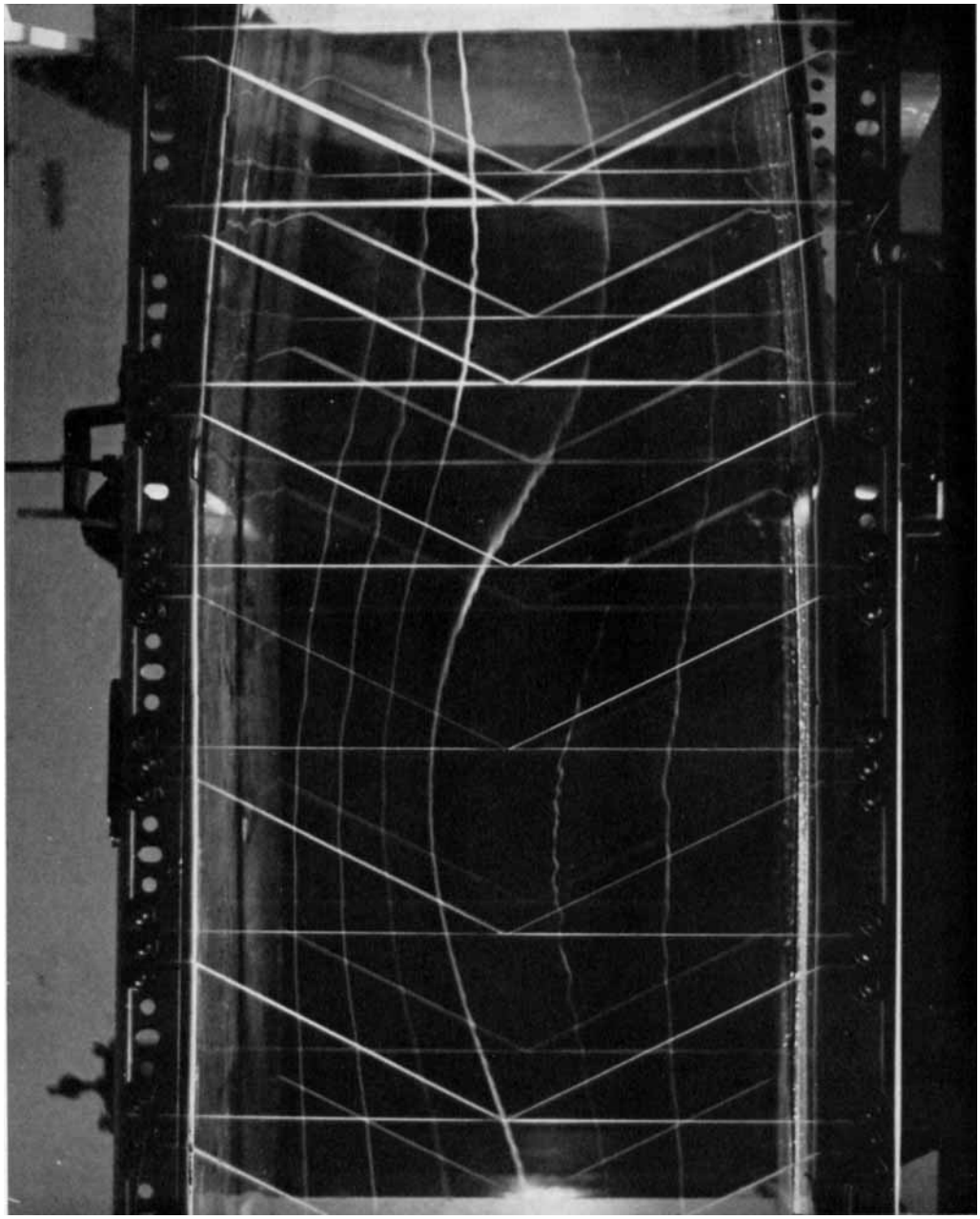

FIGURE 4. Stratified flow through a weak contraction. Near critical flow: $(F_1^2+F_2^2)_{\text{exit}} \simeq 1$.

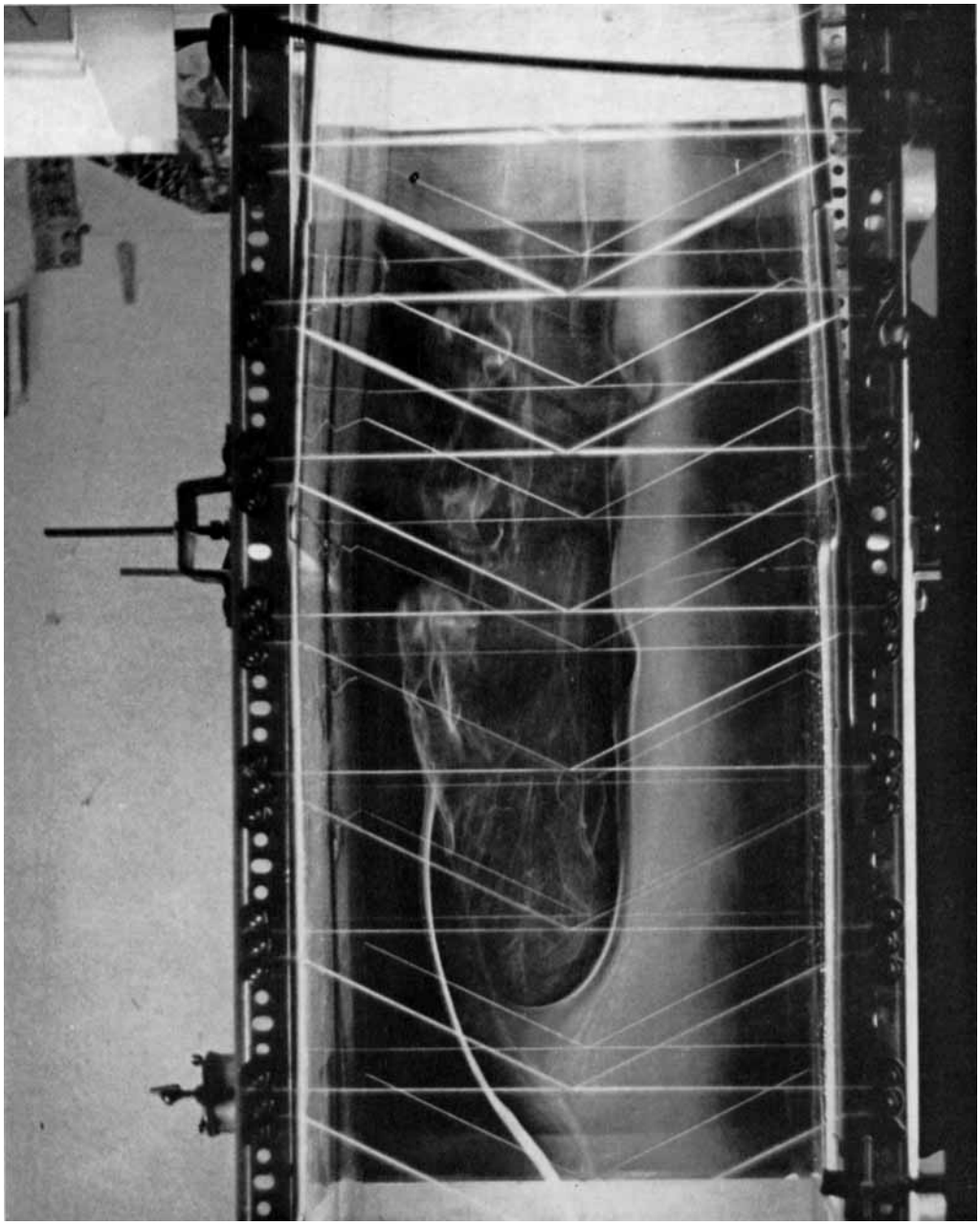

FIGURE 5. Stratified flow through a weak contraction. Subcritical flow: $(F_1^2 + F_2^2)_{\text{entrance}} < 1$.

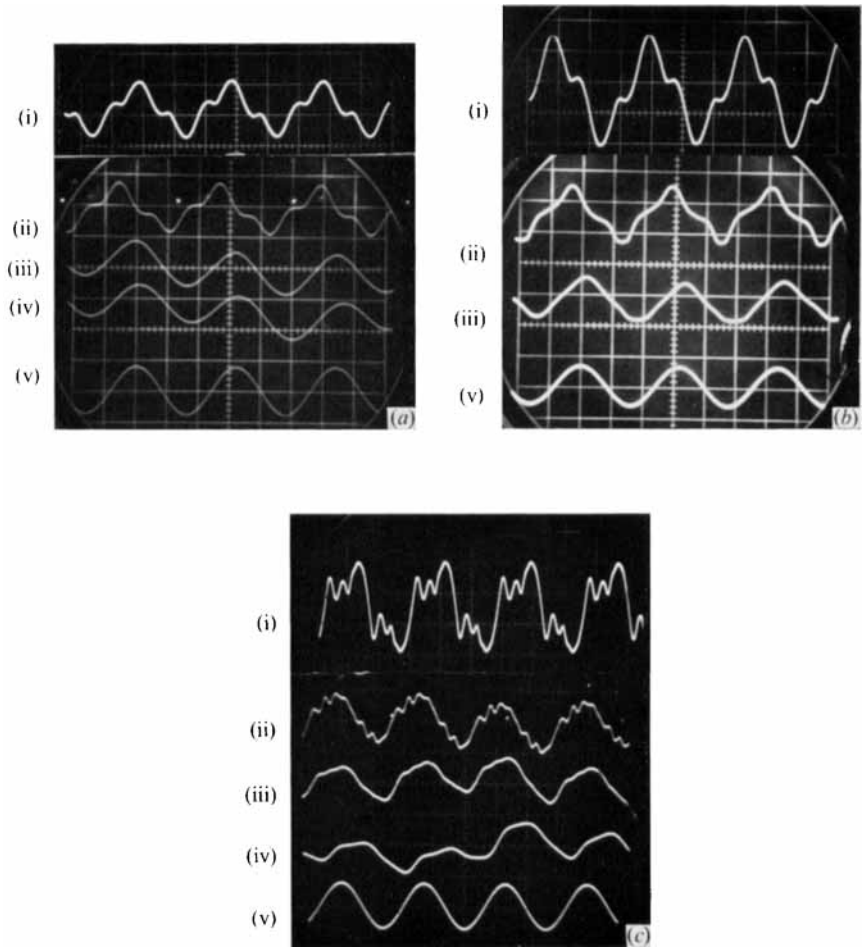

FIGURE 6. Oscilloscope traces of forced disturbance. (i) Displacement of oscillating piston; (ii) $x = 12$ in., (iii) $x = 43$, (iv) $x = 72$. (*a*) $f = 111{\cdot}2$ c/s, $\lambda = 1{\cdot}62$ in., (*b*) $f = 80{\cdot}9$, $\lambda = 2{\cdot}54$, (*c*) $f = 39{\cdot}6$, $\lambda = 4{\cdot}54$.